A Study on MoS_2 Nanolayer Coated Etched Fiber Bragg Grating Strain Sensor

S. Sridhar, Suneetha Sebastian, Ajay K. Sood, and Sundarrajan Asokan

***Abstract*—In this paper, we report on the comprehensive study on Molybdenum disulfide (MoS_2) nanolayer coated etched Fiber Bragg Grating (eFBG) strain sensor. MoS_2 nanolayer is coated using Physical Vapor Deposition (PVD) of Molybdenum (Mo) on eFBGs followed by sulfurization of the same in an inert atmosphere at 450° C. Such coating technique provides a direct control over the coating thickness of MoS_2, thereby enabling a study based on the effect of nanolayer coating thickness on the intrinsic strain sensitivity as well as the power of the back reflected Bragg wavelength of eFBG in the 0.78eV spectral region. High uniformity of MoS_2 nanolayer coating ensures consistent, repeatable and highly linear FBG strain sensors with a correlation coefficient of 0.988 in the range of 0 to 2500 $\mu\varepsilon$. A maximum intrinsic strain sensitivity of ~6.65 pm/$\mu\varepsilon$ with a resolution of ~150 nε have been achieved with optimized MoS_2 coated eFBG sensors. This kind of consistent, highly sensitive and linear strain sensors when incorporated with proper packaging schemes can be particularly useful for applications demanding high sensitivity of FBG sensors such detection of seismic vibrations, underwater acoustic signals, low amplitude accelerations, etc.**

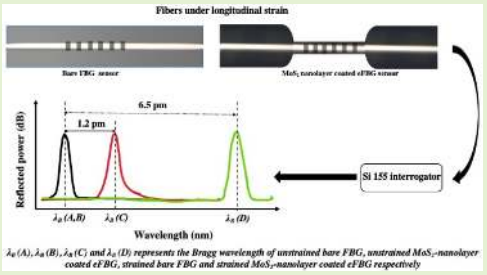

***Index Terms*— Fiber bragg grating, optical fiber sensors, strain sensors.**

I. Introduction

FIBER optic strain (FOS) sensors owing to numerous advantages, such as small size, light weight, high sensitivity, remote sensing capability and immunity to electromagnetic interference and multiplexing capability, etc., FOS have become one of the most admired sensing technologies nowadays. Rapidly growing demands have led to the concurrent development of various types of FOS sensors based on Distributed Optical Fiber sensors [1], microfiber sensors [2], Long Period Grating (LPG) [3], micro structured fibers [4], Fiber Bragg Grating (FBGs) sensor [5] etc. along with interrogation techniques such as intensity modulation [6], interferometric detection [7], wavelength detection [8] etc.

Combination of various outstanding aspects such as multifunction capability, small gauge length, ease of manipulation of the evanescent field in the sensor region, ease of incorporation with transducers; along with simple interrogation technique based on wavelength shift, has made FBGs most demanding sensors among FOS sensors. Any external perturbation, such as strain, is sensed by FBG through a shift in Bragg wavelength (λ_B) which is the reflected wavelength from the sensor. This shift in λ_B is caused by the change in effective refractive index of the fundamental mode (n_{eff}) and/or grating pitch (Λ) in the sensor portion due to the perturbations. Typically, a strain sensitivity value ~1pm/$\mu\varepsilon$ is observed in FBGs, in the operating region of 0.78 eV [9].

Improving the strain sensitivity of FBG sensors is always utmost interest to the scientists in the FOS sensing community. To date, a number of attempts have been made in this regard to increase the sensitivity of FBG sensors, either extrinsically (making use of transducers) or intrinsically (modifying the sensor region directly), to the surrounding perturbations. In the extrinsic approach, different transducers are designed

Manuscript received December 30, 2020; accepted January 10, 2021. Date of publication January 25, 2021; date of current version March 5, 2021. This work was supported in part by the Naval Research Board (NRB), Government of India, and in part by the DST-INSPIRE Faculty Scheme under Grant DST/INSPIRE/04/2017/000894. The associate editor coordinating the review of this article and approving it for publication was Prof. Agostino Iadicicco. *(S. Sridhar and Suneetha Sebastian contributed equally to this work.) (Corresponding author: Sundarrajan Asokan.)*

S. Sridhar is with the Department of Instrumentation and Applied Physics, Indian Institute of Science, Bengaluru 560012, India, and also with the Department of Physics, School Advanced Sciences, Vellore Institute of Technology, Vellore 632 014, India.

Suneetha Sebastian is with the Department of Instrumentation and Applied Physics, Indian Institute of Science, Bengaluru 560012, India, and also with the Institute of Electrical Engineering, EPFL Swiss Federal Institute of Technology, CH-1015 Lausanne, Switzerland.

Ajay K. Sood is with the Department of Physics, Indian Institute of Science, Bengaluru 560012, India.

Sundarrajan Asokan is with the Department of Instrumentation and Applied Physics, Indian Institute of Science, Bengaluru 560012, India (e-mail: sasokan@iap.iisc.ernet.in).

Digital Object Identifier 10.1109/JSEN.2021.3054473

for the purpose of improving the sensitivity of the FBG based strain sensor [10], [11]. The intrinsic approach, on the other hand, manipulates the sensor directly such as superimposing of a LPG and FBG inscribed in the same section called superimposed fiber Bragg grating (SFBG) [12], fusing of a polymer (ZEONEX-480R) FBG, in series with a silica fiber [13], etching the cladding of the FBG followed by nanomaterial coating [14] etc. The latter one has an added advantage over the former one that they can be incorporated with the transducers for further improving the sensitivity. However, at present, there are only a few works, incorporating the interdisciplinary fields of nanotechnology and FBG strain sensors for improving the sensitivity intrinsically. One such method is to etch the cladding which surrounds the core of FBG. This etching results in a strong mode coupling with the nanomaterial coating, leading to a prominent change in the effective refractive index of FBG. Also, the force/stress sensitivity of FBG depends inversely on the cross-sectional area of the fiber [15]. Thus, etched FBG (eFBG) sensors show strain sensitivity values of $\sim$2.8 pm/$\mu\varepsilon$ with a reflected Bragg wavelength value of $\sim$1545 nm whereas with reduced graphene oxide nanomaterial coating the sensitivity is 5.5 pm/$\mu\varepsilon$ [14]. Further, the sensitivity of the FBGs can be enhanced by coating a thin layer of various nanomaterials which have different refractive index value from that of the cladding; FBGs coated with numerous nanomaterials such as graphene and carbon nanotubes [3]–[5], metal or metal oxide compounds [6]–[10], various polymers and hybrid composites, such as metal particles-polymers have been reported [11], [12]. However, most of these coatings are processed by dip coating and sol-gel method and their coating thicknesses vary in the range of few hundreds of nm [14], [16] and even though the works show an improved sensitivity, controlling the coating thickness and the uniformity of coating remains as a real challenge.

Recently, Molybdenum disulfide (MoS_2) semiconductor which belong to the group of transition metal dichalcogenides (TMDCs) family are being widely studied because of their impressive mechanical and optical properties, high gauge factor and tunable band gap [17]. MoS_2 is considered as 'beyond graphene' due to its direct bandgap nature which will compensate for the gapless nature of graphene and find extensive applications as nano-electromechanical sensors [18], piezo-resistive strain sensors [19], tactile sensor [17], etc. Tuning the bandgap of MoS_2 with applied strain is a promising capability of the material which provides additional opto-electronic properties to the material [20]. Due to these superior properties, recently MoS_2 nanolayer coated fiber sensor systems have been used for different sensing applications [21]–[24].

In the present work, we demonstrate that MoS_2 nanolayer coated eFBGs can serve as highly sensitive strain sensors. Sputter coating of Mo onto eFBG followed by sulfurization yielded MoS_2 nanolayer coated eFBG sensors. The formation of the MoS_2 coating on the fiber surface is confirmed using X-ray photoelectron spectroscopy (XPS) analysis. This superior coating technique on fiber surface, eliminates the tedious and complex process of surface modification of the fiber prior to nanomaterial coating [14]. Also, the method provides a direct control over the coating thickness of the material to a few nanometers which is studied using Atomic Force Microscopy (AFM). A maximum intrinsic strain sensitivity of $\sim$6.65 pm/$\mu\varepsilon$ is observed for $\sim$9 nm MoS_2 nanolayer coated eFBG sensors in the range of 0 to 2500 $\mu\varepsilon$, which is almost six times higher strain sensitive as compared to bare FBG sensors.

TABLE I
PARAMETERS USED FOR MO COATING BY SPUTTERING

Parameter	Value
Target Material	Mo
Temperature	Room Temperature
Distance	5 cm
Base Pressure	2×10^{-5} mbar
Deposition Pressure	0.05 mbar
Power	10 W
Ar flow rate	5 sccm
Pre-deposition time	10 min
Deposition time	5, 10, 20 and 30 sec

II. MATERIALS AND METHODS

A. Sensor Fabrication

In this work, FBGs are fabricated in single mode photo sensitive optical fibers (Nufern, GF1) with core and clad thicknesses of around 8 μm and 125 μm respectively. The FBGs are inscribed in the fiber using the phase mask method, employing a KrF excimer laser with a power of 3.8 mJ and a repetition rate of 200 Hz. Following grating inscription, the cladding of the sensor has been etched, such that the final diameter of the sensor is around 9 μm, using a standard chemical etching process described elsewhere [25]. Subsequently, the etched fibers are coated with the nanolayer of MoS_2. This entire process of coating of MoS_2 over the fiber has been conducted in two steps. In the first step, the eFBGs are placed in to the sputtering chamber for the uniform, ultra-thin layer of Molybdenum (Mo) coating. In the second step, such Mo coated eFBGs are shifted to a quartz tubular furnace for sulfurization.

Mo thin films are coated on eFBG sensor using a commercial DC magnetron sputtering system. Molybdenum (Mo) powder (Alfa Aesar, purity 99.95%) is made into 2-inch pallet (diameter: 2″, thickness: 3 mm) and is used as sputtering target. Since the etched sensors are very fragile due to the reduction in their diameter ($\sim$9 μm), special clamps have been employed, to hold the fiber thereby preventing it from breaking. The eFBG sensors are then introduced into the vacuum chamber of the sputtering system and placed at a distance of 5 cm away from the Mo target. The vacuum chamber is initially evacuated to a base pressure of 2×10.5 mbar. Subsequently, Argon (99.999% pure) with the flow rate of 5 sccm is introduced into the chamber and the working gas pressure during the film deposition is maintained at 0.05 mbar. The DC power supply is then turned ON and kept at 10 W for all the coatings. The coating parameters are summarized in Table I.

TABLE II
DESIGNATION, SPUTTER DEPOSITION TIME, SULFURIZATION TIME AND COATING THICKNESS OBTAINED FROM AFM IMAGES OF MoS_2 SAMPLES

Designation	Deposition time of Mo (s)	Sulfurization time (hrs)	Coating thickness (nm)
MoS_2_5	5	24	3
MoS_2_10	10	24	5
MoS_2_20	20	24	7
MoS_2_30	30	24	9

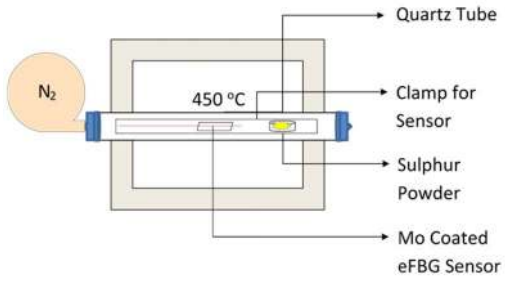

Fig. 1. Schematic of sulfurization process of Mo coated eFBG optical sensors.

In order to confirm the uniform coating thickness on both sides of the clamp (sensor), the coating process is repeated on the other side as well. Four samples of Mo coated eFBGs have been fabricated with varying the deposition times as shown in Table.II.

Lastly, Mo coated eFBGs (with different deposition times of Mo) are transferred into a quartz tubular furnace for sulfurization of Mo. The tubular furnace, which contains Mo coated eFBG sensors and sulfur powder in a crucible, is evacuated first in order to remove the atmospheric oxygen present in it; then it is purged with an inert gas (N_2) to create an inert atmosphere. This process of evacuation and purging of inert gas, is repeated several times to confirm the inert atmosphere inside the tube. The furnace is subsequently heated up to 450 °C at a rate of 2 °C/min and kept at 450 °C for 24 hrs and cooled down to room temperature naturally. The process of sulfurization of Mo could be perceived from fig. 1. All samples have been subjected to sulfurization for the same duration.

B. Experimental Setup

The sensors, MoS_2 coated eFBGs, are then placed on a Carbon Fiber Reinforced Polymer (CFRP) rod (28× 3.5 × 0.3 cm) which serves as a cantilever for measuring the strain sensitivity. The tensile strain developed in the rod by adding calibrated weights at the free end is measured using a Resistance Strain Gauge (RSG) connected to a Data Acquisition System. In order to ensure better accuracy in the measurements, the sensor is properly fixed on the CFRP rod by means of an appropriate gluing material. The change in λ_B corresponding to the strain in the rod has been recorded using Micron Optics Interrogator system (si155) having 1 pm resolution and data acquisition rate of 5 kHz.

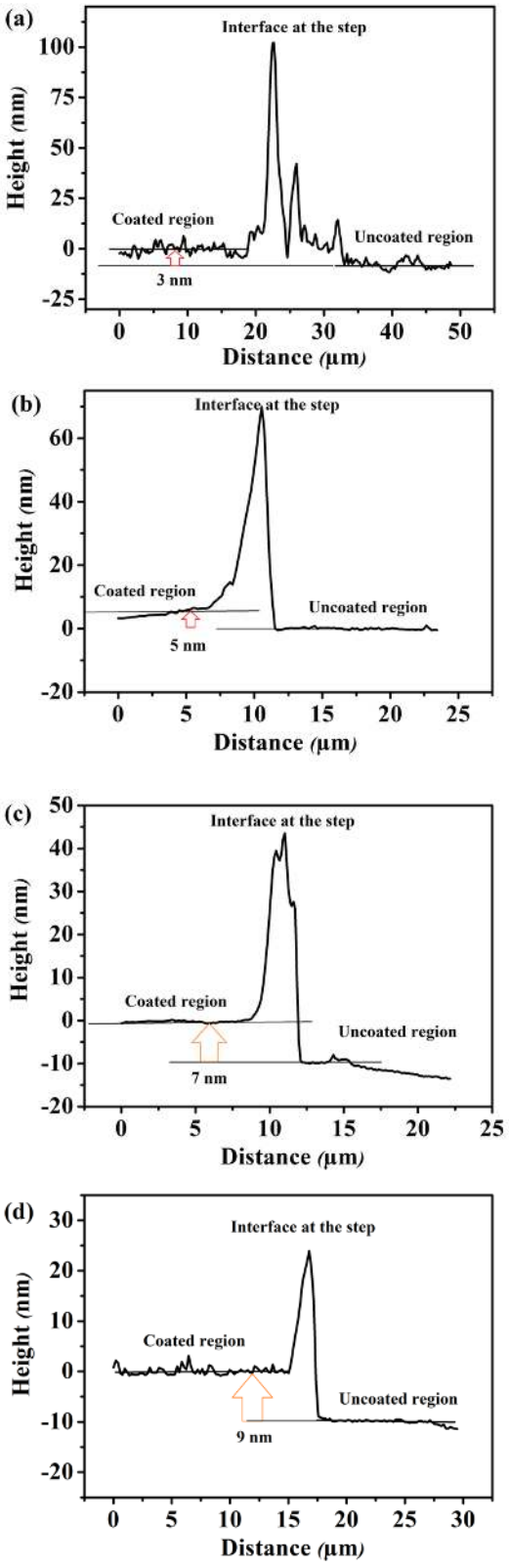

Fig. 2. AFM height profile of MoS_2 coated samples with varying sputter deposition time (a) 5 sec (b) 10sec (c) 20 sec and (d) 30 sec.

C. Sensor Characterizations

All sensors are characterized properly to find the thickness of MoS_2 coating prior to the strain experiment, using Atomic Force Microscopy (AFM). Fig. 2 shows the AFM

height profile of all sensors under consideration. To measure the precise height (thickness) of coating in comparison with the substrate surface, a thin strip of tape is stuck on the fiber surface. Once the coating is done, the tape is carefully removed such that a height profile (step) is created between the uncoated and coated region of the fiber. Conversely, the interface between the fiber and the tape has comparatively high deposition rate hence a hump is observed at the interface. In order to measure the thickness precisely, the humpy region at the interface is ignored and the readings are taken farther away from the interface. The height difference between the coated and uncoated regions (as shown in fig.2) will precisely give the quantitative measurement of the thickness of the nanomaterial coating.

It can be seen that with different deposition times, of Mo onto the surface of the samples along with a constant sulfurization time yields varying thickness. Table.II shows that a variation from around 3 nm to 9 nm is observed as the time of Mo deposition is varied from 5 s to 30 s. Since atomically thin single layer of MoS_2 has a thickness around 0.625 nm, coating thickness of MoS_2 around 3 nm, yields a total number of layers of around 5.

X-ray photoelectron spectroscopy (XPS) analysis has been performed on the as synthesized MoS_2_30 sample (shown in fig.3) in order to confirm the successful formation of MoS_2 and to obtain the quantitative information of the various species present on the surface.

For this, Mo has been sputter coated on to a silicon wafer substrate and further sulfurized in the tube furnace with the same conditions used for coating over FBGs. Fig. 3(a) shows the wide range spectrum of XPS profile obtained for MoS_2/SiO_2 film which confirms the presence of surface Mo, S, C, and O atoms. The binding energies of Mo and S atom are measured from Fig. 3(b) and (c). Mo 3d peaks at 228.55 eV and 231.69 eV are attributed to the doublet of Mo $3d_{5/2}$ and Mo $3d_{3/2}$ of MoS_2, respectively [26], [27]. Apart from these two primary peaks, there are peaks at 228.73 and 231.95 eV which are due to the formation of MoS_xO_y and are attributed to the doublet of Mo $3d_{5/2}$ and Mo $3d_{3/2}$ of MoS_xO_y [28]. Also, sulphur atom-related 2S peak is observed at 226.11 eV. S^{2-} peaks are also observed (Fig. 3(c)) at 162.64 and 164.48 eV due to S $2p_{1/2}$ and S $2p_{3/2}$, respectively. In addition, a peak at 235.01 eV which corresponds to the Mo^{6+} of MoO_3 is observed. The oxygen attached to the as-grown MoS_2 film can be resulting from the interfacial Mo-oxide layer due to Mo-oxygen bonding at the MoS_2-SiO_2 interface and due the presence of moisture [29]. The atomic percentage of Mo and S atoms present in the as-grown Mo_xS_y is calculated from the Mo 3d and S2p peaks (shown in Table. III) of the wide spectrum; the atomic percentage has been found as Mo 33.46% and S 66.54% which confirms the formation of MoS_2.

D. Analysis of Effective Refractive Index Dependence on Cladding Diameter

MoS_2 coated on eFBGs are of a few nanometers in thickness as shown from fig.2. The change in initial value of λ_B from bare FBG to MoS_2_30 is monitored during the experiment

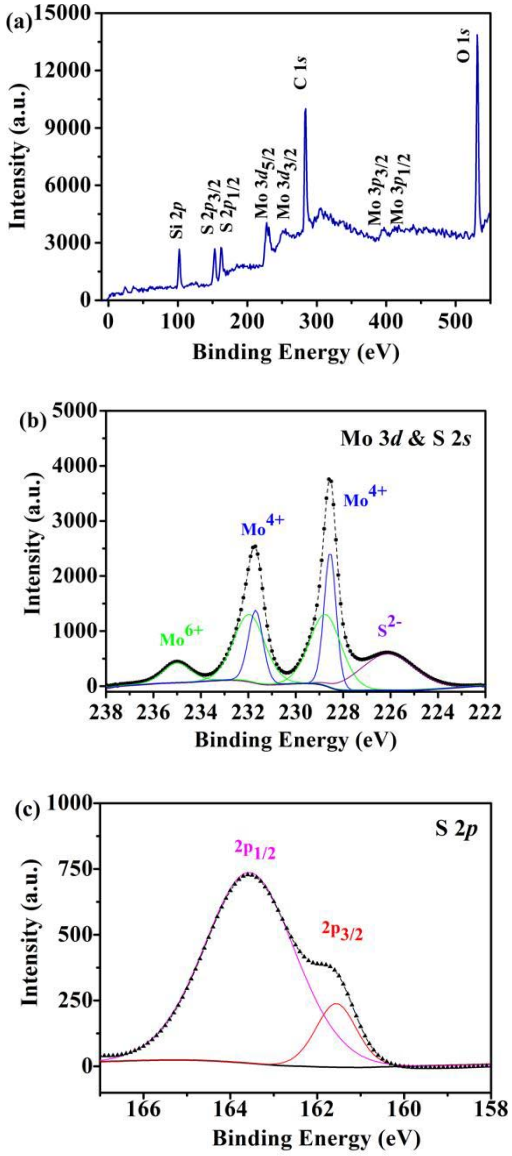

Fig. 3. (a) Wide range XPS spectrum obtained for MoS_2 sample confirms the presence of Mo, S, C, and *O* atoms (b) the fitted Mo 3d core level spectra of MoS_2 and (c) the fitted *S* 2p core level spectra of MoS_2.

TABLE III
PARAMETERS USED FOR CALCULATING THE RATIO OF MO & *S*

Name	Position (eV)	FWHM	Area	Atomic %
S 2p	163.13	3.37	151.60	66.54
Mo 3d	229.13	7.22	431.77	33.46

using the Si 155 interrogator. With coating of nanolayers of Mo onto eFBG, Bragg wavelength is red shifted to ∼500 pm from its initial value. This shift becomes much more prominent with nanolayer MoS_2 coating which comes to ∼3.5 nm.

Etching of cladding around the fiber core enables the interaction of guided mode in the core to the external perturbations through evanescent field. Modification of the complex effective refractive index in single mode fiber during etching

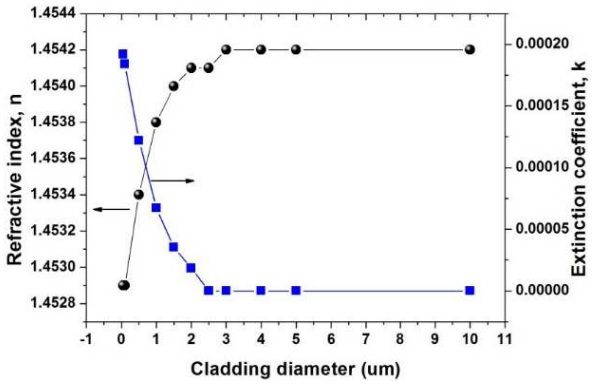

Fig. 4. Variation of effective complex refractive index of the guided mode with cladding diameter.

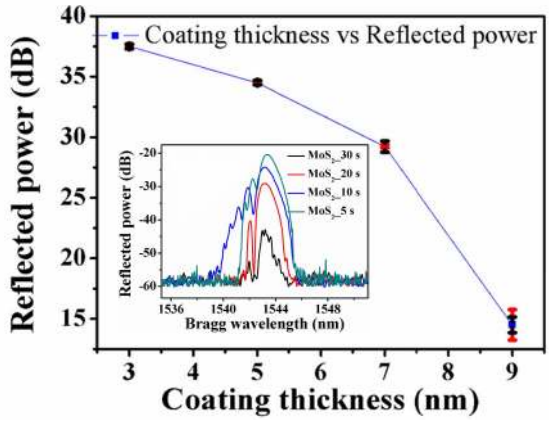

Fig. 5. Variation in reflected power of MoS_2 coated eFBGs with varying thickness. The inset shows the spectra of (a) MoS_2_5, (b) MoS_2_10, (c) MoS_2_20 and (d) MoS_2_30. The peak in the spectra corresponds to λ_B.

is solved using the electromagnetic module in the COMSOL Multiphysics software. When the clad is etched up to 2.5 μm, n_{eff} of the guided fundamental mode (LP_{01}) is unchanged (fig.4) as shown already in a previous work [30]. However, as the etching is progressed beyond this thickness, n_{eff} starts becoming complex with real part (known as refractive index, n) decreasing and the imaginary part (known as extinction coefficient (k)) increasing. k represents the attenuation of the electric field intensity of the guided mode outside the fiber core. This attenuated field is the evanescent field which will interact with the surrounding perturbations and it comes into picture as the cladding is removed below 2.5 μm from its initial value of 125 μm. It can be seen from fig.4 that, n decreases from 1.4542 to 1.4529 whereas the extinction coefficient increases from 0 to 2×10^{-4}, when the cladding is fully removed. Thus, optical absorption coefficient (α) and penetration depth calculated from k value for a clad etched fiber are found to be 500 nm^{-1} and 2000 nm respectively in the 0.78eV region. Therefore, this calculation gives a theoretical estimation of the nanomaterial coating thickness for an effective interaction of the evanescent field with nanostructures. Thus, a nanomaterial coating thickness below 2000 nm is preferred over the clad etched fibers for the effective light matter interaction.

III. Results and Discussions

A. Strain Measurements

In the present case, nanolayers of MoS_2 has a refractive index around 4.2 in the 0.78eV region [31] whereas eFBG has an effective refractive index of 1.453 in the same region. This high refractive index contrast between the eFBG and MoS_2 nanolayer can be detrimental to the guidance of fundamental mode through the structure. But as reported earlier [32], guidance through the fiber is still possible in this high contrast scenario provided the thickness of the coating should be less than λ/4n, in this case which comes around 90 nm. As of now, a proper explanation pertaining to this phenomenon of light propagation has not been given convincingly. As can be seen from fig.5, light guidance is observed, in the present high refractive index contrast case, up to a certain thickness of nanomaterial coating as reported earlier [32]. The power of the reflected λ_B from MoS_2 coated eFBG for a thickness of 3 nm is around 37 dBm and diminishes with coating thickness and reflection becomes nearly zero when the thickness of coating is greater than 9 nm. This optimized thickness up to which light propagation in this high refractive index contrast regime is found to be around 9 nm for a etched fiber thickness of around 9 μm. Thus, the coating thickness determines the signal strength/reflected power of the etched FBGs.

Further, nanolayer MoS_2 coated eFBGs of different nanomaterial coating diameter is subjected to a tensile strain through the cantilever setup as explained earlier. Under strain, the Bragg wavelength of MoS_2 coated eFBGs changes and this change seems to be higher than that of bare FBG (1.2 pm/$\mu\varepsilon$) and etched FBG (2.8 pm/$\mu\varepsilon$). Fig. 6 shows the strain sensitivity of MoS_2 coated eFBG, having different coating thickness. For sensors, MoS_2_5, MoS_2_10, MoS_2_20 and MoS_2_30, the strain sensitivity is found to be 5.84 pm/$\mu\varepsilon$, 5.93 pm/$\mu\varepsilon$, 6.05 pm/$\mu\varepsilon$ and 6.65 pm/$\mu\varepsilon$ respectively. It is found that with increase in nanolayer thickness, sensitivity also increases. The linearity of the strain response curves in the range of 0 to 2500 $\mu\varepsilon$ has a correlation coefficient, R, of 0.988 over the entire measurement region. A consistent result has been noticed in all individual cases with maximum strain sensitivity of 6.65 pm/$\mu\varepsilon$ for a 9 nm coating thickness. This enhanced intrinsic sensitivity of nanolayer MoS_2 coated eFBG sensors can be attributed to the optical bandgap dependency of the MoS_2 nanolayers on the tensile strain thereby making the refractive index of the material as a function of tensile strain [33-34]. Thus, it is assumed that when the refractive index of MoS_2 nanolayers becomes matching with that of effective refractive index of the fiber fundamental mode, light interaction begins with nanolayers. Due to this interaction of the guided mode, the effective refractive index of the mode may get modified each time under different strains along with usual strain-optic effect. Shift in Bragg wavelength ($\Delta\lambda_B$) of a bare FBG sensor due to the applied strain is given by [35],

$$\Delta\lambda_B = \lambda_B(1 - \rho_e)\varepsilon \quad (1)$$

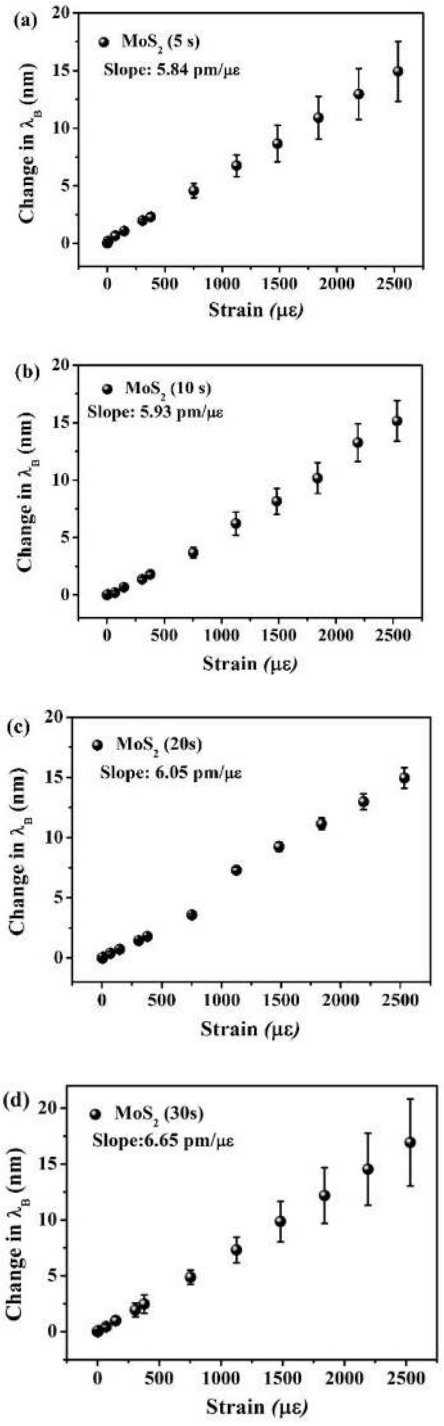

Fig. 6. Change in Bragg wavelength with applied strain for eFBGs coated with nanolayer of MoS_2 with varying coating thickness (a) MoS_2_5, (b) MoS_2_10, (c) MoS_2_20 and (d) MoS_2_30.

where, λ_B is the initial Bragg wavelength, ρ_e is the strain optic coefficient and ε is the applied longitudinal strain. Corresponding change in refractive index (Δn) of bare FBG sensor for the an applied longitudinal strain is given as

$$\Delta n = -\frac{1}{2} n^3 \left[\varepsilon (1-\nu) P_{12} - \nu \varepsilon P_{11}\right] \quad (2)$$

where n is the refractive index of the fiber with zero strain, ε is the applied longitudinal strain, ν is the Poisson's ratio of fiber, P_{11} and P_{12} are the coefficients of strain optic tensor. Thus, it can be assumed that the presence of MoS_2 nanolayer coating, modifies equation (2) with a term relative to refractive index change of MoS_2 under the same strain ($n_{MoS2}(\varepsilon)$). So, such a kind of combined contribution to refractive index variation of the fundamental mode along with pitch variation of the sensor changes $\Delta\lambda_B$ (given in equation (1)) otherwise under tensile strain and may result in high strain sensitivity. A detailed theoretical study on this phenomenon of strain enhancement using nanolayer MoS_2 coating on eFBGs will be carried in the future.

TABLE IV
COMPARISON OF STRAIN SENSITIVITY OBTAINED FOR FBG SENSORS BY DIFFERENT METHODS

Materials/Design	Sensitivity (pm/με)	Reference
Intrinsic:		
Bare FBG	1.2	[37]
Polyimide coated FBG	1.82	[38]
eFBG	2.8	[14]
RGO coated eFBG	5.5	[14]
MoS_2 coated eFBG	6.65	Present work
Type I FBG	1.2	[39]
Pre-strained FBG	1.32	[39]
Extrinsic:		
FBG integrated on a lever structure.	5.2	[11]
Flexible hinge bridge	10.84	[10]
SFBG	13.01	[12]

IV. CONCLUSION

A two-step fabrication method of sputtering with Mo followed by sulfurization is adopted for coating nanolayers of MoS_2 onto eFBG sensors. With this method of deposition, highly uniform and reproducible nanolayer coating on eFBGs has been attained. The nanolayer coating thickness on sensors has been varied with different deposition times of Mo, keeping time of sulfurization a constant. It has been observed that the reflected signal power from FBG sensors gets diminished with respect to coating thickness and the propagation of light through the sensor is observed up to a nanolayer coating thickness of around 9 nm in the present high refractive index contrast regime. A maximum strain sensitivity of nearly 6.65pm/$\mu\varepsilon$ is observed for 9 nm of MoS_2 nanolayer coating on eFBG sensors, which is much higher than that of bare FBG sensors. Even though the diameter of the nanolayer coating has no much significance in terms increase in intrinsic strain sensitivity of the sensor, the coating thickness will determine the strength of light reflection from the sensor which becomes quite significant when such sensors are subjected to different packaging schemes. Such a study based on effect of coating thickness on the intrinsic strain sensitivity and back reflected optical signal power of eFBG sensors is reported for the first time, to the best of our knowledge. The present work demonstrates highest intrinsic strain sensitivity of FBG sensors, as compared to all other existing FBG sensors (mentioned in the table IV). This kind of sensors along with a proper packaging, such as described in [36], can be used for a variety of applications which demand high sensitivity of the sensors.

ACKNOWLEDGMENT

The authors would also like to thank MNCF, CeNSE, Indian Institute of Science, for FESEM, XPS and Raman Scattering analysis and SERC, Indian Institute of Science, for technical support for implementing COMSOL simulations. Dr. S. Sebastian would like to thank Prof. Dr. L. Thévenaz (Group for Fibre Optics, Institute of Electrical Engineering, EPFL, Switzerland) for the opportunity to work in his lab and for offering his supervision. Dr. Sridhar S would like to express his thanks to UGC for the financial assistance.

REFERENCES

[1] L. Costa, H. F. Martins, S. Martín-López, M. R. Fernández-Ruiz, and M. González-Herráez, "Fully distributed optical fiber strain sensor with 10^{-12} $\epsilon/\sqrt{\text{Hz}}$ sensitivity," *J. Lightw. Technol.*, vol. 37, no. 18, pp. 4487–4495, Sep. 15, 2019.

[2] K. Li, J. Wang, and T. Guo, "Optical microfiber sensors," in *Advanced Fiber Sensing Technologies* (Progress in Optical Science and Photonics), vol. 9, L. Wei, Ed. Singapore: Springer, 2020.

[3] L. Madhavan and M. Chattopadhyay, "Temperature and strain sensitivity of long period grating fiber sensor," *Int. J. Res. Eng. Technol.*, vol. 4, no. 2, pp. 776–782, 2015.

[4] G. Durana, J. Gomez, G. Aldabaldetreku, J. Zubia, A. Montero, and I. S. de Ocariz, "Assessment of an LPG mPOF for strain sensing," *IEEE Sensors J.*, vol. 12, no. 8, pp. 2668–2673, Aug. 2012.

[5] Q. Chen *et al.*, "A method of strain measurement based on fiber Bragg grating sensors," *Vibroeng. Procedia*, vol. 5, pp. 140–144, Sep. 2015.

[6] J. Hu *et al.*, "A high sensitive fiber-optic strain sensor with tunable temperature sensitivity for temperature-compensation measurement," *Sci. Rep.*, vol. 7, no. 1, p. 42430, Mar. 2017.

[7] H. Chen, S. Zhang, H. Fu, B. Zhou, and N. Chen, "Sensing interrogation technique for fiber-optic interferometer type of sensors based on a single-passband RF filter," *Opt. Exp.*, vol. 24, no. 3, pp. 2765–2773, 2016.

[8] A. Prasad, S. Sebastian, and S. Asokan, "Diaphragm-micro-stylus-based fiber Bragg grating tactile sensor," *IEEE Sensors J.*, vol. 20, no. 12, pp. 6394–6399, Jun. 2020.

[9] S. W. James and R. P. Tatam, "Optical fibre long-period grating sensors: Characteristics and application," *Meas. Sci. Technol.*, vol. 14, no. 5, pp. R49–R61, May 2003.

[10] M. Liu, W. Wang, H. Song, S. Zhou, and W. Zhou, "A high sensitivity FBG strain sensor based on flexible hinge," *Sensors*, vol. 19, no. 8, p. 1931, Apr. 2019.

[11] R. Li, Y. Chen, Y. Tan, Z. Zhou, T. Li, and J. Mao, "Sensitivity enhancement of FBG-based strain sensor," *Sensors*, vol. 18, no. 5, p. 1607, May 2018.

[12] G. Guo, "Superstructure fiber Bragg gratings for simultaneous temperature and strain measurement," *Optik*, vol. 182, pp. 331–340, Apr. 2019.

[13] R. Oliveira, L. Bilro, T. H. R. Marques, C. M. B. Cordeiro, and R. Nogueira, "Strain sensitivity enhancement of a sensing head based on ZEONEX polymer FBG in series with silica fiber," *J. Lightw. Technol.*, vol. 36, no. 22, pp. 5106–5112, Nov. 15, 2018.

[14] K. S. Vasu, S. Asokan, and A. K. Sood, "Enhanced strain and temperature sensing by reduced graphene oxide coated etched fiber Bragg gratings," *Opt. Lett.*, vol. 41, no. 11, pp. 2604–2607, 2016.

[15] G. Rajan, B. Liu, Y. Luo, E. Ambikairajah, and G.-D. Peng, "High sensitivity force and pressure measurements using etched singlemode polymer fiber Bragg gratings," *IEEE Sensors J.*, vol. 13, no. 5, pp. 1794–1800, May 2013.

[16] E. Davies, R. Viitala, M. Salomäki, S. Areva, L. Zhang, and I. Bennion, "Sol–gel derived coating applied to long-period gratings for enhanced refractive index sensing properties," *J. Opt. A: Pure Appl. Opt.*, vol. 11, no. 1, 2009, Art. no. 015501.

[17] M. Park, Y. J. Park, X. Chen, Y.-K. Park, M.-S. Kim, and J.-H. Ahn, "MoS_2-based tactile sensor for electronic skin applications," *Adv. Mater.*, vol. 28, no. 13, pp. 2556–2562, Apr. 2016.

[18] W. Wei, J. Nong, L. Tang, N. Wang, C.-J. Chuang, and Y. Huang, "Graphene-MoS_2 hybrid structure enhanced fiber optic surface plasmon resonance sensor," *Plasmonics*, vol. 12, no. 4, pp. 1205–1212, 2017.

[19] M.-Y. Tsai *et al.*, "Flexible MoS_2 field-effect transistors for gate-tunable piezoresistive strain sensors," *ACS Appl. Mater. Interfaces*, vol. 7, no. 23, pp. 12850–12855, 2015.

[20] H. J. Conley, B. Wang, J. I. Ziegler, R. F. Haglund, Jr., T. S. Pantelides, and K. I. Bolotin, "Bandgap engineering of strained monolayer and bilayer MoS_2," *Nano Lett.*, vol. 13, no. 8, pp. 3626–3630, Aug. 2013.

[21] C. Li, X. Peng, C. Wang, S. Cao, and H. Zhang, "Few-layer MoS_2-deposited flexible side-polished fiber Bragg grating bending sensor for pulse detection," in *Proc. 19th Int. Conf. Solid-State Sensors, Actuat. Microsyst. (TRANSDUCERS)*, 2017, pp. 2007–2010.

[22] S. Sebastian, S. Sridhar, R. A. Jilin, S. A. V. Varu, A. Sreejith, and S. Asokan, "Multilayer MoS_2 coated etched fiber Bragg grating based hydrophone," in *Proc. IEEE SENSORS*, Oct. 2018, pp. 1–3.

[23] S. Sridhar, S. Sebastian, and S. Asokan, "Temperature sensor based on multi-layer MoS_2 coated etched fiber Bragg grating," *Appl. Opt.*, vol. 58, no. 3, pp. 535–539, 2019.

[24] B. Du *et al.*, "MoS_2-based all-fiber humidity sensor for monitoring human breath with fast response and recovery," *Sens. Actuators B, Chem.*, vol. 251, pp. 180–184, Nov. 2017.

[25] P. Beccat, P. Da Silva, Y. Huiban, and S. Kasztelan, "Quantitative surface analysis by XPS: Application to hydro-treating catalysts; Analyse quantitative de surface par XPS (X-ray photoelectron spectroscopy): Application aux catalyseurs d'hydrotraitement," *Oil Gas Sci. Technol.*, vol. 54, no. 4, pp. 487–496, 1999.

[26] B. S. Kavitha, N. K. Radhika, S. S. Gorthi, and S. Asokan, "Etched fiber Bragg grating sensor for quantification of DNA," *IEEE Sensors J.*, vol. 21, no. 2, pp. 1588–1595, Jan. 2021, doi: 10.1109/JSEN.2020.3020943.

[27] S. Hussain *et al.*, "Large-area, continuous and high electrical performances of bilayer to few layers MoS_2 fabricated by RF sputtering via post-deposition annealing method," *Sci. Rep.*, vol. 6, no. 1, p. 30791, Aug. 2016.

[28] A. D. Gandubert, C. Legens, D. Guillaume, S. Rebours, and E. Payen, "X-ray photoelectron spectroscopy surface quantification of sulfided CoMoP catalysts–relation between activity and promoted sites–Part I: Influence of the Co/Mo ratio," *Oil Gas Science Technol.*, vol. 62, no. 1, pp. 79–89, 2007.

[29] X. Zhao and S. S. Perry, "The role of water in modifying friction within MoS2 sliding interfaces," *ACS Appl. Mater. Interfaces*, vol. 2, no. 5, pp. 1444–1448, May 2010.

[30] R. Mudachathi, B. N. Shivananju, G. R. Prashanth, S. Asokan, and M. M. Varma, "Calibration of etched fiber Bragg grating sensor arrays for measurement of molecular surface adsorption," *J. Lightw. Technol.*, vol. 31, no. 14, pp. 2400–2406, Jul. 15, 2013.

[31] H.-L. Liu, C.-C. Shen, S.-H. Su, C.-L. Hsu, M.-Y. Li, and L.-J. Li, "Optical properties of monolayer transition metal dichalcogenides probed by spectroscopic ellipsometry," *Appl. Phys. Lett.*, vol. 105, no. 20, Nov. 2014, Art. no. 201905.

[32] Z. L. Poole, P. Ohodnicki, R. Chen, Y. Lin, and K. P. Chen, "Engineering metal oxide nanostructures for the fiber optic sensor platform," *Opt. Exp.*, vol. 22, no. 3, pp. 2665–2674, 2014.

[33] A. Castellanos-Gomez *et al.*, "Local strain engineering in atomically thin MoS_2," *Nano Lett.*, vol. 13, no. 11, pp. 5361–5366, 2013.

[34] N. M. Ravindra, P. Ganapathy, and J. Choi, "Energy gap–refractive index relations in semiconductors–an overview," *Infr. Phys. Technol.*, vol. 50, no. 1, pp. 21–29, Mar. 2007.

[35] K. O. Hill and G. Meltz, "Fiber Bragg grating technology fundamentals and overview," *J. Lightw. Technol.*, vol. 15, no. 8, pp. 1263–1276, Aug. 1997.

[36] S. Sebastion, S. Sridhar, P. S. Prasad, and S. Asokan, "Highly sensitive fiber Bragg grating-based pressure sensor using side-hole packaging," *Appl. Opt.*, vol. 58, no. 1, pp. 115–121, Jan. 2019.

[37] Y. J. Rao, "In-fibre Bragg grating sensors," *Meas. Sci. Technol.*, vol. 8, no. 4, p. 355, 1997.

[38] J. Jung, H. Nam, B. Lee, J. O. Byun, and N. S. Kim, "Fiber Bragg grating temperature sensor with controllable sensitivity," *Appl. Opt.*, vol. 38, no. 13, pp. 2752–2754, 1999.

[39] A. Rahman and S. Asokan, "Fiber Bragg grating sensors: New ideas on strain-temperature discrimination," *Int. J. Smart Sens. Intell. Syst.*, vol. 3, no. 1, pp. 108–117, 2010.

S. Sridhar received the bachelor's and master's degrees in physics, and the M.Sc.Engg. and Ph.D. degrees from the Department of Instrumentation and Applied Physics, Indian Institute of Science, Bengaluru, India. He qualified for UGC-CSIR Junior Research Fellowship (JRF) and National Eligibility Test (NET) in 2012. He is currently working as an Assistant Professor (Senior) with the Department of Physics, School of Advanced science, VIT University, Vellore Campus, India.

Suneetha Sebastian received the Ph.D. degree from the International School of Photonics, Cochin University of Science and Technology (CUSAT), India, in 2016. She was a National-Post Doctoral Fellow (funded by the Department of Science and Technology (DST), Government of India) at the Department of Instrumentation and Applied Physics, Indian Institute of Science, Bengaluru, India, from 2016 to 2017. She joined the Department of Instrumentation and Applied Physics as DST-INSPIRE Faculty, awarded by the Government of India, in 2017. She is currently working as a Visiting Faculty/Researcher with the Group for Fiber Optics, Institute of Electrical Engineering, Swiss Federal Institute of Technology at Lausanne (EPFL), Switzerland.

Ajay K. Sood received the Ph.D. degree from the Indian Institute of Science, Bengaluru, in 1982. After postdoctoral research at the Max-Planck Institute in Stuttgart, he served in IGCAR for a short time. Then, he joined IISc, Bengaluru, in 1988, where he continues to serve till now. He is currently an Honorary Professor with the Department of Physics, IISc. Over three decades in IISc, he has served in various capacities including as the Chairman, Division of Physical and Mathematical Sciences from 1998 to 2008. Further, he has been honored with a number of prestigious awards and honors. At the national level, he has served as Member for various advisory councils such as, Scientific Advisory Council to the Prime Minister of India (2009–2014), Member, Science and Engineering Research Board (SERB) (2012-2014) etc. to name a few. Also, he served as the President of the Indian Academy of Sciences (2010-2012), Indian National Science Academy, and as a Secretary General, Third World Academy of Sciences (TWAS) (2013-18). He is an elected Fellow of all the three National Science Academies in India and The World Academy of Sciences (TWAS). In 2015, he was elected as a Fellow of the Royal Society (FRS) London. In recognition of his scientific contributions and service to science in India, he has been honoured with “Padma Shri” by the Government of India in 2013.

Sundarrajan Asokan received the Ph.D. degree in physics from Indian Institute of Science, Bengaluru, India. He was a JSPS Visiting Scientist with the Department of Electronics and Computer Engineering, Gifu University, Gifu, Japan, in 1991, and a Visiting Scholar with the Lyman Laboratory, Harvard University, Cambridge, MA, USA, in 1999. He is currently the Chairman and MSIL Chair Professor of the Department of Instrumentation and Applied Physics, Indian Institute of Science. He has edited two books and published more than 210 articles in international journals/books. He has been a Fellow of the National Academy of Sciences, India, since 2008. He was a recipient of The Martin J. Forster Gold Medal from the Indian Institute of Science for the Best Ph.D. Thesis in the Division of Physical and Mathematical Sciences for the year 1986–1987, the Young Scientist Award of the Indian National Science Academy (1990), and the Young Scientist Research Award of the Department of Atomic Energy (1995), India, and the INSA-Royal Society Visiting Scientist award from the Imperial College of Science, Technology and Medicine, London, U.K., in 1998. He has been elected as a Fellow of the National Academy of Sciences, India, in 2008.